MODELLING AND ALLOCATION OF A DSTATCOM ON THE PERFORMANCE IMPROVEMENT OF UNBALANCED RADIAL DISTRIBUTION SYSTEMS

Padarbinda. SAMAL[1], Sanjeeb. MOHANTY[2], Sanjib. GANGULY[3]
[1, 2] Department of Electrical Engineering, National Institute of Technology, Rourkela, India-769008
[3]Department of Electronics and Electrical Engineering, Indian Institute of Technology Guwahati
[1]Corresponding author's email: padarbindasamal87@gmail.com

Abstract: *In this paper a three phase modelling of DSTATCOM has been carried out for unbalanced radial distribution systems. Further the modelled DSTATCOM has been incorporated in the load flow algorithm and placed at each bus of distribution systems one at a time except the source bus. The placement of the DSTATCOM clearly indicates that system power loss decreases and the voltage profile improvement takes place with respect to base case. A 25 bus system and a 19-bus unbalanced radial distribution systems are considered as the test systems.*

Key words*: Unbalanced radial distribution systems, three phase modelling, distribution static synchronous compensator, load flow.*

1. Introduction

The distribution system is considered to be a lossy system due to high R/X ratio of the distribution lines, and the low operating voltage. Moreover, the distribution systems suffer various power quality issues such overvoltage, undervoltage, harmonic distortion, etc. This in turn reduces the operational efficiency, the service quality, and the reliability of distribution systems. In recent times, the custom power devices such as distribution static synchronous compensator (DSTATCOM) [1] are considered as the best tool to alleviate all the power quality problems. In all of the works, the DSTATCOM is allocated in balanced radial distribution systems and its impact on the system performance is studied [2-14]. The particle swarm based optimization was employed to obtain the optimal location and size of distributed generations and DSTATCOM for minimizing the system power loss [2]. Jazebi *et. al*. [3] implemented differential evolution algorithm considering network reconfiguration so as to minimize the power loss distribution networks. The authors in [4] utilized bacterial foraging algorithm in order to reduce the power loss, the total operational cost, and the voltage profile index of distribution systems. Salman *et. al* [5] proposed binary gravitation search algorithm to minimize the voltage sag in a distribution system. In [6], an analytic method was applied in minimizing the total system power loss and minimum voltage magnitude. Farhoodnea *et. al* [7] employed firefly algorithm for optimizing the average voltage total harmonic distortion, average voltage deviation, and total investment cost. Tolabi *et. al* [8] proposed fuzzy ant colony optimization for minimizing the system loss, increasing load balancing index, and voltage profile of a system by simultaneous reconfiguration, optimal allocation of DSTATCOM and photovoltaic array. The impact of distributed generator on the allocation and size of DSTATCOM was investigated in [9]. Here, the total cost of DSTATCOM was considered the objective function to be minimized. Jain *et. al.* [10] applied voltage stability index method in order to obtain the optimal location of DSTATCOM. The minimization of real power loss was chosen as the objective function. In [11], a fuzzy shuffled frog-leaping algorithm was developed so as to reduce the total power loss, equal load balancing index, and voltage deviation by reconfiguring the network in presence of capacitors, and DSTATCOM. Taher and Afsari implemented [12] an optimization algorithm called the immune algorithm in order to minimize the power loss and size of the DSTATCOM. Xiaoguang *et. al.* [13] have used genetic algorithm for obtaining the optimal network configuration for minimizing the total cost of the system with the help of DSTATCOM and dynamic voltage restorer. In [14], a meta-heuristic algorithm called bat algorithm was applied to minimize the system power loss. However, no works have been reported for the optimal placement and sizing of

DSTATCOM in unbalanced radial distribution systems. Moreover three-phase modelling of the DSTATCOM is not carried out by any researchers.

In this work, a three-phase modelling of DSTATCOM is developed. The proposed DSTATCOM is allocated in unbalanced radial distribution systems for power loss minimization. The simulation results obtained with a 25-bus and 19-bus systems show that significant amount of power loss reduction is obtained by suitably placing the DSTATCOM in the system.

The paper is organized as follows: In Section 2, a three-phase DSTATCOM model is described. The incorporation of DSTATCOM in the three phase-unbalanced load flow is presented in Section 3. The simulation results are discussed in Section 4. Section 5 concludes the paper.

2. Three-phase modelling of DSTATCOM

A three phase three wire line section model including a DSTATCOM between bus *i* and bus *j* is shown in Fig. 1. The parameters of the line can be obtained by Carson and Lewis [15] technique. The impedance matrix consisting of both self and mutual impedances are derived from [15].

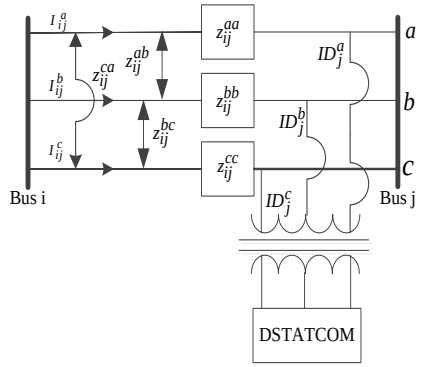

Fig. 1. Dstatcom installation in bus j in a three-phase three wire line section model

Where, z_{ij}^{aa}, z_{ij}^{bb}, and z_{ij}^{cc} denotes self impedance of phase a, phase b, and phase c respectively; z_{ij}^{ab}, z_{ij}^{bc}, and z_{ij}^{ca} denotes mutual impedance between phases.

Applying Kirchhoff's voltage law (KVL) equation in between bus i and bus j when DSTATCOM is connected at bus j in Fig.1. We obtain the equation as follows:

$$\begin{bmatrix} V_j^a\angle(\alpha_1) \\ V_j^b\angle(-120^0+\alpha_2) \\ V_j^c\angle(120^0+\alpha_3) \end{bmatrix} = \begin{bmatrix} V_i^a\angle\delta_1 \\ V_i^b\angle\delta_2 \\ V_i^c\angle\delta_3 \end{bmatrix} - \begin{bmatrix} Z_{ij}^{aa} & Z_{ij}^{ab} & Z_{ij}^{ac} \\ Z_{ij}^{ba} & Z_{ij}^{bb} & Z_{ij}^{bc} \\ Z_{ij}^{ca} & Z_{ij}^{cb} & Z_{ij}^{cc-n} \end{bmatrix} \begin{bmatrix} IL_j^a\angle\theta_a \\ IL_j^b\angle\theta_b \\ IL_j^c\angle\theta_c \end{bmatrix} - \begin{bmatrix} Z_{ij}^{aa} & Z_{ij}^{ab} & Z_{ij}^{ac} \\ Z_{ij}^{ba} & Z_{ij}^{bb} & Z_{ij}^{bc} \\ Z_{ij}^{ca} & Z_{ij}^{cb} & Z_{ij}^{cc} \end{bmatrix} \begin{bmatrix} ID_j^a\angle(\alpha_1+\pi/2) \\ ID_j^b\angle(\alpha_2+\pi/2-120^0) \\ ID_j^c\angle(\alpha_3+\pi/2+120^0) \end{bmatrix} \quad (1)$$

Where ID_j^a , ID_j^b , and ID_j^c are the current injected by DSTATCOM at phase a, b, and c respectively.

Simplifying the equation (1) as follows:

$$\begin{bmatrix} V_j^a\angle(\alpha_1) \\ V_j^b\angle(-120^0+\alpha_2) \\ V_j^c\angle(120^0+\alpha_3) \end{bmatrix} = \begin{bmatrix} V_i^a\angle\delta_1 \\ V_i^b\angle\delta_2 \\ V_i^c\angle\delta_3 \end{bmatrix} - \begin{bmatrix} Z_{ij}^{aa}IL_j^a\angle\theta_a + Z_{ij}^{ab}IL_j^b\angle\theta_b + Z_{ij}^{ac}IL_j^c\angle\theta_c \\ Z_{ij}^{ba}IL_j^a\angle\theta_a + Z_{ij}^{bb}IL_j^b\angle\theta_b + Z_{ij}^{bc}IL_j^c\angle\theta_c \\ Z_{ij}^{ca}IL_j^a\angle\theta_a + Z_{ij}^{cb}IL_j^b\angle\theta_b + Z_{ij}^{cc}IL_j^c\angle\theta_c \end{bmatrix} - \quad (2)$$

$$\begin{bmatrix} Z_{ij}^{aa}ID_j^a\angle(\alpha_1+\pi/2)+Z_{ij}^{ab}ID_j^b\angle(\alpha_2+\pi/2-120^0)+Z_{ij}^{ac}ID_j^c\angle(\alpha_3+\pi/2+120^0) \\ Z_{ij}^{ba}ID_j^a\angle(\alpha_1+\pi/2)+Z_{ij}^{bb}ID_j^b\angle(\alpha_2+\pi/2-120^0)+Z_{ij}^{bc}ID_j^c\angle(\alpha_3+\pi/2+120^0) \\ Z_{ij}^{ca}ID_j^a\angle(\alpha_1+\pi/2)+Z_{ij}^{cb}ID_j^b\angle(\alpha_2+\pi/2-120^0)+Z_{ij}^{cc}ID_j^c\angle(\alpha_3+\pi/2+120^0) \end{bmatrix}$$

Simplifying eq. (2) for phase a, we obtain:

$$V_j^a\cos\alpha_1 = \mathrm{Real}(V_i^a\angle\delta_1) - \mathrm{Real}(Z_{ij}^{aa}IL_j^a\angle\theta_a + Z_{ij}^{ab}IL_j^b\angle\theta_b + Z_{ij}^{ac}IL_j^c\angle\theta_c) - \mathrm{Real}(Z_{ij}^{aa}ID_j^a\angle(\alpha_1+\pi/2) + Z_{ij}^{ab}ID_j^b\angle(\alpha_2+\pi/2-120^0) + Z_{ij}^{ac}ID_j^c\angle(\alpha_3+\pi/2+120^0)) \quad (3)$$

$$V_j^a\sin\alpha_1 = \mathrm{Imag}(V_i^a\angle\delta_1) - \mathrm{Imag}(Z_{ij}^{aa}IL_j^a\angle\theta_a + Z_{ij}^{ab}IL_j^b\angle\theta_b + Z_{ij}^{ac-n}IL_j^c\angle\theta_c) - \mathrm{Imag}(Z_{ij}^{aa}ID_j^a\angle(\alpha_1+\pi/2) + Z_{ij}^{ab}ID_j^b\angle(\alpha_2+\pi/2-120^0) + Z_{ij}^{ac}ID_j^c\angle(\alpha_3+\pi/2+120^0)) \quad (4)$$

Let,

$$a1 = \mathrm{Real}(V_i^a\angle\delta_1) - \mathrm{Real}(Z_{ij}^{aa}IL_j^a\angle\theta_a + Z_{ij}^{ab}IL_j^b\angle\theta_b + Z_{ij}^{ac}IL_j^c\angle\theta_c)$$

$$a2 = \mathrm{Imag}(V_i^a\angle\delta_1) - \mathrm{Imag}(Z_{ij}^{aa}IL_j^a\angle\theta_a + Z_{ij}^{ab}IL_j^b\angle\theta_b + Z_{ij}^{ac}IL_j^c\angle\theta_c)$$

Let, $b = V_j^a$, $b1 = V_j^b$,and $b2 = V_j^c$ (5)

$$b\sin\alpha_1 = a2 + ID_j^a(k3\cos\alpha_1 - k4\sin\alpha_1) + ID_j^b(k9\cos(-120^0+\alpha_2) - k10\sin(-120^0+\alpha_2)) + ID_j^c(k11\cos(120^0+\alpha_3) - k12\sin(120^0+\alpha_3)) \quad (6)$$

Adding equation (5) and (6)

$$b\cos\alpha_1 + b\sin\alpha_1 = a1 + a2 + ID_j^a(k1\cos\alpha_1 + k2\sin\alpha_1) + ID_j^b(k5\cos(-120^0+\alpha_2) + k6\sin(-120^0+\alpha_2)) + ID_j^c(k7\cos(120^0+\alpha_3) + k8\sin(120^0+\alpha_3)) + ID_j^a(k3\cos\alpha_1 - k4\sin\alpha_1) + ID_j^b(k9\cos(-120^0+\alpha_2) - k10\sin(-120^0+\alpha_2)) + ID_j^c(k11\cos(120^0+\alpha_3) - k12\sin(120^0+\alpha_3)) \quad (7)$$

Simplifying equation (7)

$$b(\cos\alpha_1+\sin\alpha_1)=a1+a2+[ID_j^a(\cos\alpha_1(k1+k3)+\sin\alpha_1(k2-k4))+ ID_j^b(\cos(-120^0+\alpha_2)*(k5+k9)+\sin(-120^0+\alpha_2)*(k2-k8))+ ID_j^c(\cos(120^0+\alpha_3)*(k7+k11)+\sin(120^0+\alpha_3))*(k8-k12)] \quad (8)$$

Again simplifying eq. (8)

$$b(\cos\alpha_1+\sin\alpha_1)=a1+a2+[ID_j^a(\cos\alpha_1.(ka)+\sin\alpha_1.(kb))+ID_j^b(\cos(-120^0+\alpha_2).(kc)+ \sin(-120^0+\alpha_2).(kd))+ID_j^c(\cos(120^0+\alpha_3).(ke)+\sin(120^0+\alpha_3)).(kf)] \quad (9)$$

Similarly for phase b

$$b1(\cos(-120^0+\alpha_2)+\sin(-120^0+\alpha_2))=a3+a4+[ID_j^a(\cos\alpha_1.(kg)+\sin\alpha_1.(ki))+ ID_j^b(\cos(-120^0+\alpha_2).(kj)+\sin(-120^0+\alpha_2).(km))+ID_j^c(\cos(120^0+\alpha_3).(kn) +\sin(120^0+\alpha_3)).(ko)] \quad (10)$$

Similarly for phase c

$$b2(\cos(120^0+\alpha_2)+\sin(120^0+\alpha_2))=a3+a4+[ID_j^a(\cos\alpha_1.(kp)+\sin\alpha_1.(kr))+ ID_j^b(\cos(-120^0+\alpha_2).(ks)+\sin(-120^0+\alpha_2).(kt))+ID_j^c(\cos(120^0+\alpha_3).(ku) +\sin(120^0+\alpha_3)).(kv)] \quad (11)$$

Solving eq. (8)-eq. (10) simultaneously for different values of α_1, α_2, α_3 we can obtain the values of DSTATCOM current magnitudes ID_j^a, ID_j^b, and ID_j^c respectively.

The range of α_1, α_2, α_3 are assumed as:

$$0<\alpha_1<1 \quad (12)$$

$$0<\alpha_2<1 \quad (13)$$

$$0<\alpha_3<1 \quad (14)$$

The reactive power that must be injected by the DSTATCOM at phase a, b, and c is expressed below:

$$jQ_{DSTAT}^a=(V_j^a\angle\alpha_1).(ID_j^a\angle(\alpha_1+\pi/2))^* \quad (15)$$

$$jQ_{DSTAT}^b=(V_j^b\angle\alpha_2).(ID_j^b\angle(\alpha_2+\pi/2))^* \quad (16)$$

$$jQ_{DSTAT}^c=(V_j^c\angle\alpha_3).(ID_j^c\angle(\alpha_3+\pi/2))^* \quad (17)$$

It can be observed that DSTATCOM is injecting current in quadrature with the bus voltage where it is connected so as to compensate the reactive power only. This is explained in a phasor diagram as shown in Fig. 2.

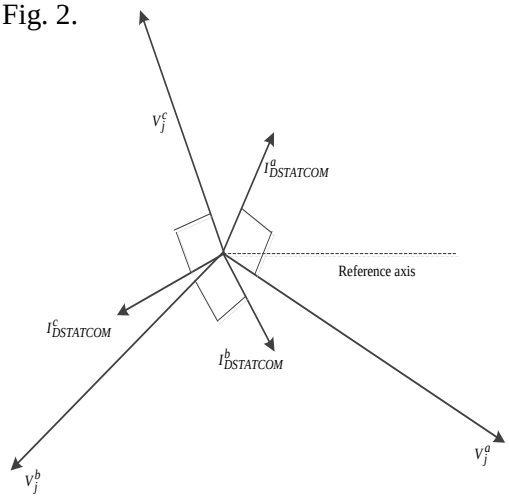

Fig. 2. Phasor diagram of dstatcom currents with respect to voltages at phase a, b, and c, respectively

3. Incorporation of DSTATCOM in Load Flow

The load flow [16] algorithm is used to find the total real power loss, and the voltage at buses of unbalanced radial distribution systems. This load flow algorithm basically consists of two steps. In the first step, backward sweep is executed to find out the branch currents. Then, the forward sweep is executed to obtain the bus voltages.

The modelling of the three-phase DSTATCOM for the unbalanced distribution systems have three unknown parameters namely, α_1, α_2, α_3. Where, α_1 is defined as the angular displacement of voltage at phase a at the location where a DSTATCOM is connected. Similarly, α_2 and α_3 can be defined. Here, three different values of α_1, α_2, and α_3 are considered for obtaining the current injected by DSATCOM at phase a, phase b, and phase c for 25-bus and 19-bus system respectively. However the values of α_1, α_2, and α_3 may be different for 25-bus and 19-bus systems. This may be due different reactive power requirements of both the systems. Fig. 3. shows the flow chart of the load flow algorithm in which the DSTATCOM model is included.

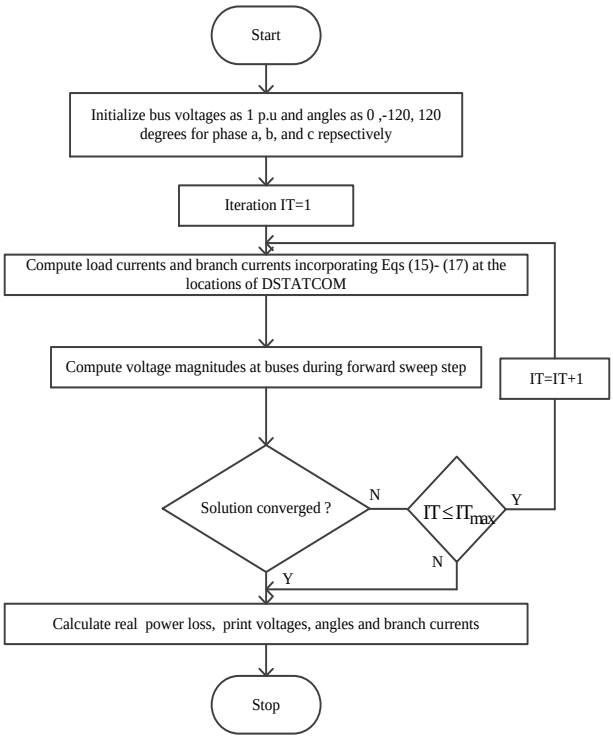

Fig . 3. Flow chart of forward backward sweep load flow algorithm including the DSTATCOM model

4. Simulation results and Discussion

The computer simulation is performed in order to demonstrate the effect of DSTATCOM allocation on two test systems, i.e., an 25-bus and a 19-bus unbalanced radial distribution systems.

4.1. Effect of DSTATCOM allocation on the system power loss and voltage profile for 25-bus system. The network diagram of 25-bus URDS is depicted in Fig. 4. The base kV and base MVA for 25-bus system is taken as 4.16 kV and base MVA is considered as 30 MVA. The results for 25-bus system for different case studies is shown in Table 1. The load and conductor data are provide in Table A1 and A2 in the appendix respectively. The base case power loss of this system is 150.12 kW.

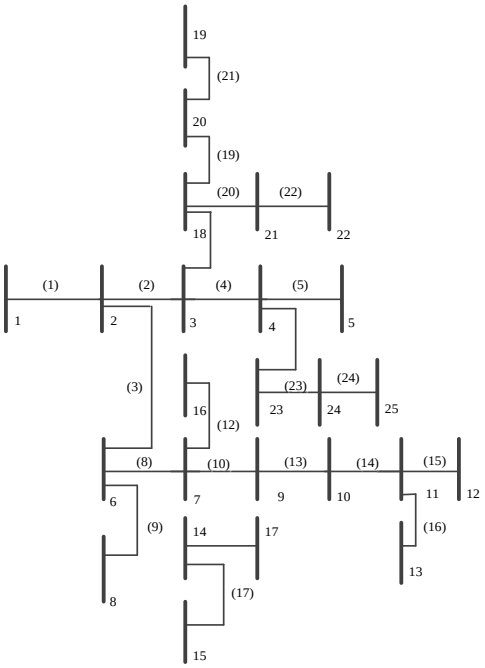

Fig.4. A 25-bus URDS, (a) 1,2,3…,25 denotes bus number ; (b) (1), (2),(3),…,(24) denotes branch numbers (c) All the branches are considered three phase lines

Table 1: Results obtained with DSTATCOM for 25-bus system for different cases

Location	Case	α (Degree)			KVA Rating			Real power loss(kW)	Power loss reduction in (%)
		Phase a	Phase b	Phase c	Phase a	Phase b	Phase c		
15	A	-0.1	0.8	0.8	173.903	34.213	61.807	136.5427	9.04
	B	0.1	0.5	0.3	261.089	37.454	34.487	135.7396	9.58
	C	0.1	0.2	0.5	270.703	35.287	42.169	135.2793	9.89

The DSATCOM is placed at each bus except the source one at a time, and the power loss for the different cases is shown in Fig. 5. A significant reduction in power loss is observed when DSTATCOM is connected at bus 11 and bus 15. However, highest power loss reduction is observed at bus 15. The power loss versus DSTATOCM Location graph for all the case studies follow a similar pattern.

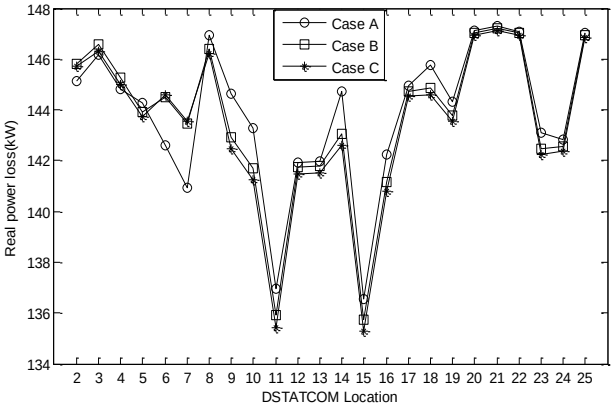

Fig. 5. Real power loss after DSTATCOM allocation in URDS

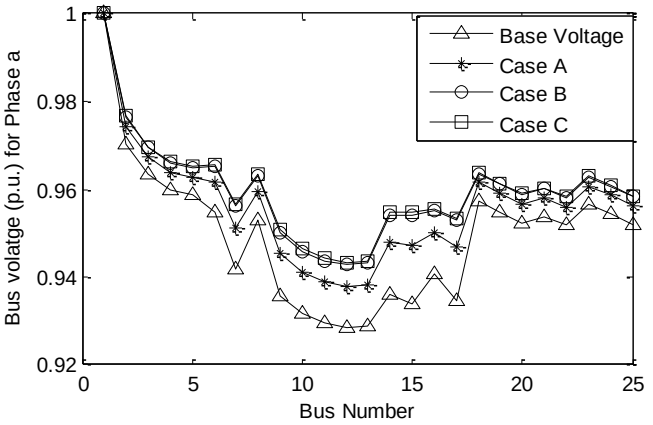

Fig. 6. Voltage magnitude for phase a corresponding to different cases with DSTATCOM at Bus 15

The voltage profile of the 25-bus system corresponding to different cases for the phase a is shown in Fig. 6. The voltage magnitude for Case C is found to be higher than other cases. This may be due to the reason that reactive power injection for the Case C is higher than Case B, Case A.

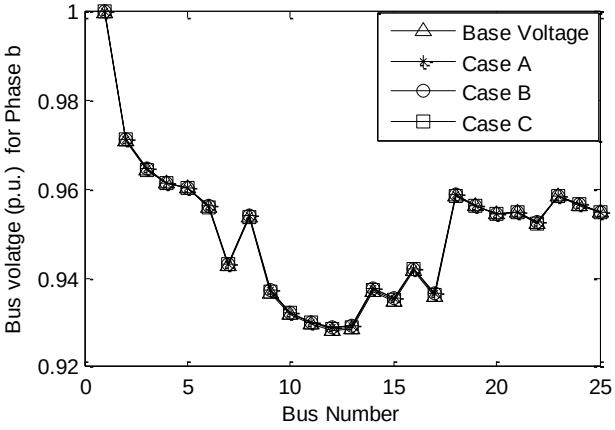

Fig.7. Voltage magnitude for phase b corresponding to different cases with DSTATCOM at Bus 15

From Fig. 7 and 8 a slight improvement in voltage magnitudes for Case C, Case B, and Case A is observed in comparison to base case as the reactive power injected at phase b, and phase c is found to be much lower than injected at phase a.

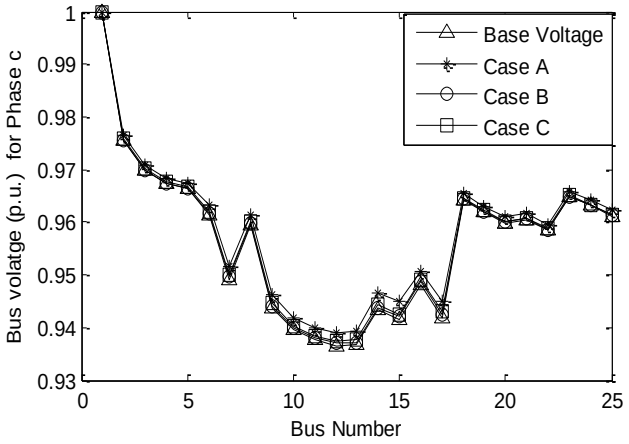

Fig. 8. Voltage magnitude for phase c corresponding to different cases with DSTATCOM at Bus 15

4.2. Effect of DSTATCOM allocation on the system power loss and voltage profile for 19-bus system

Fig. 9 shows the network diagram of a 19-bus system. The base case values for 19-bus system are considered to be 11kV and base MVA as 1. The base case power loss of 19-bus system is 13.47 kW. The results for 19-bus system for different case studies is shown in Table 2. The load and conductor data are provide in Table A3 and A4 in the appendix respectively.

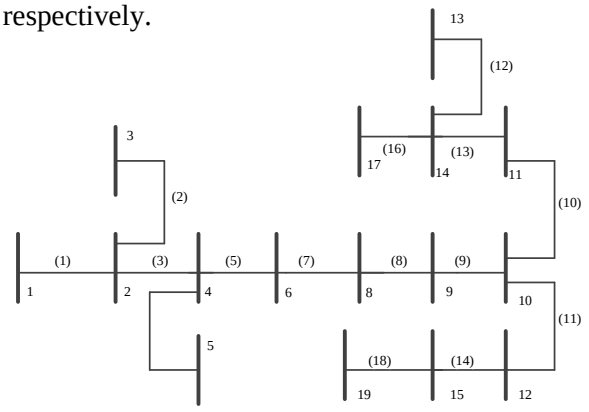

Fig. 9. A 19-bus URDS, (a) 1,2,3…,19 denotes bus number (b) (1), (2),(3),…,(18) denotes branch numbers (c) All the branches are considered three phase lines

The DSATCOM is placed at each bus except the source one at a time, and the power loss for the different cases is shown in Fig. 10. It is observed that total system power loss is found to minimum when DSTATCOM is placed at bus number 11.

Table 2: Results obtained with DSTATCOM for 19-bus system for different cases

Location	Case	α (Degree)			KVA Rating			Real power loss	Power loss reduction in (%)
		Phase a	Phase b	Phase c	Phase a	Phase b	Phase c		
11	A	0.12	0.1	0.12	28.018	29.652	10.514	11.7378	10.14
	B	0.1	0.2	0.2	36.683	36.233	15.721	11.5186	15.64
	C	0.21	0.15	0.2	37.400	37.623	39.899	11.1169	17.22

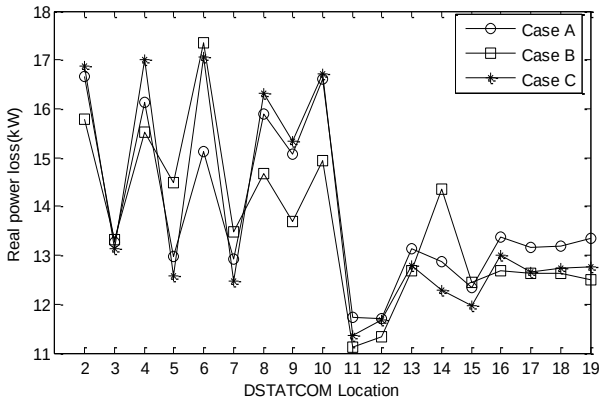

Fig. 10. Real power loss after allocation of DSTATCOM in URDS

Fig. 11. depicts the voltage profile of the 19-bus system for different cases for phase a when DSTATCOM is placed at bus 11. It is observed that voltage magnitude at all buses for Case A, Case B, Case C has improved in comparison to base case.

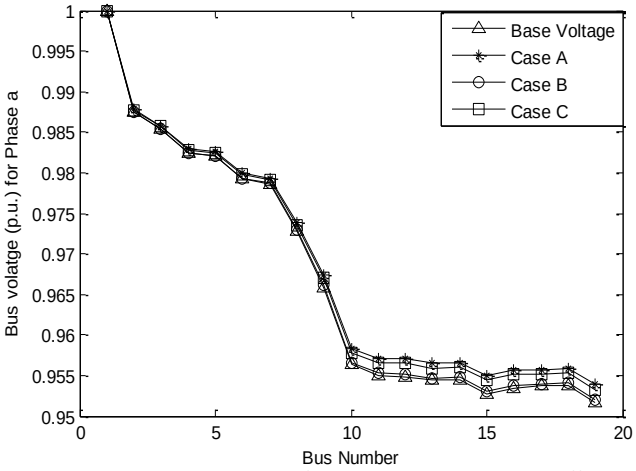

Fig. 11. Voltage magnitude for phase a corresponding to different cases with DSTATCOM at Bus 11

The voltage magnitude at all buses of the 19-bus system for phase b, when DSTATCOM is placed at bus number 11 is shown in Fig. 12. A significant improvement in voltage magnitude at buses is observed for Case A and B with respect to base case values.

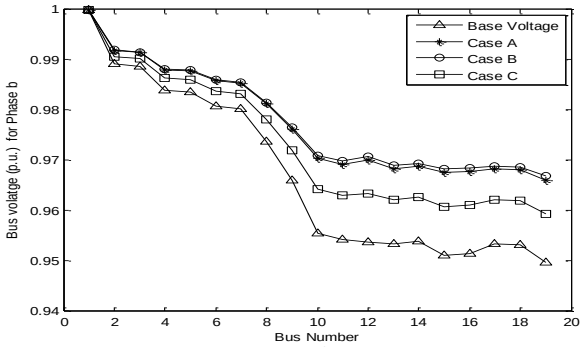

Fig. 12. Voltage magnitude for phase b corresponding to different cases with DSTATCOM at Bus 11

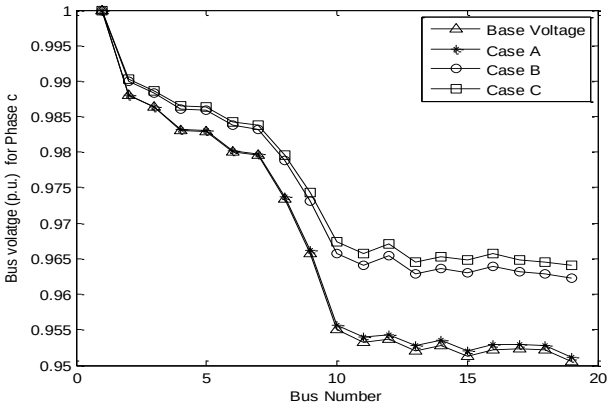

Fig. 13. Voltage magnitude for phase c corresponding to different cases with DSTATCOM at Bus 11

In Fig. 13, the voltage magnitude of all buses for phase c for 19-bus system is shown. It is clearly seen that voltage magnitudes at all buses for Case C and Case B has improved considerably in comparison to base case value when DSATCOM is placed at bus number 11 of 19-bus system.

5. Conclusion

This paper presents the impact of a DSTATCOM allocation in URDS. A three phase modelling of DSTATCOM has been developed. The power loss and voltage magnitude at each bus placing one at a time, except source bus is calculated by incorporating the DSTATCOM in a three phase load flow algorithm. Simulation results depict that significant amount of power loss is reduced due to allocation of DSTATCOM. However, only few locations are found to effective in view of power loss reduction and voltage profile improvement.

References

[1] Farhoodnea, M., Mohamed, A., Shareef, H., Zayandehroodi, H.: ‘A Comprehensive Review of Optimization Techniques Applied for Placement and Sizing of Custom Power Devices in Distribution Networks’PRZEGLĄD ELEKTROTECHNICZNY (Electrical Rev., 2012, (11), pp. 261–265.

[2] Devi, S., Geethanjali, M.: ‘Optimal location and sizing determination of Distributed Generation and DSTATCOM using Particle Swarm Optimization algorithm’Int. J. Electr. Power Energy Syst., 2014, 62, pp. 562–570.

[3] Jazebi, S., Hosseinian, S.H., Vahidi, B.: ‘DSTATCOM allocation in distribution networks considering reconfiguration using differential evolution algorithm’Energy Convers. Manag., 2011, 52, (7), pp. 2777–2783.

[4] K. Ravi, K.R.D.: ‘Optimal size and siting of multip le DG and DSTATCOM in radial distribution system using Bacterial Foraging Optimization Algorithm’Ain Shams Eng. J., 2015, pp. 1–13.

[5] Nesrullah, S., Azah, M., Hussain, S.: ‘Reliability Improvement in Distribution Systems by Optimal Placement of DSTATCOM Using Binary Gravitational Search Algorithm’Przegl Ąd Elektrotechniczny (Electrical Rev., 2012, 88, (2), pp. 295–299.

[6] Hussain, S.M.S., Subbaramiah, M.: ‘An analytical approach for optimal location of DSTATCOM in radial distribution system’, in ‘2013 International Conference on Energy Efficient Technologies for Sustainability’ (2013), pp. 1365–1369

[7] Farhoodnea, M., Mohamed, A., Shareef, H., Zayandehroodi, H.: ‘Optimum D-STATCOM placement using firefly algorithm for power quality enhancement’, in ‘Power Engineering and Optimization Conference (PEOCO), 2013 IEEE 7th International’ (2013), pp. 98–102

[8] Tolabi, H.B., Ali, M.H., Member, S., Rizwan, M.: ‘Simultaneous Reconfiguration , Optimal Placement of DSTATCOM , and Photovoltaic Array in a Distribution System Based on Fuzzy-ACO Approach’IEEE Trans. Sustain. Energyustainable Energy, 2015, 6, (1), pp. 210–218.

[9] Eldery, M.A., El-Saadany, E.F., Salama, M.M.A.: ‘Effect of distributed generator on the allocation D-STATCOM in distribution network’, in ‘Power Engineering Society General Meeting, 2005. IEEE’ (2005), pp. 2360–2364 Vol. 3

[10] Jain, A., Gupta, A.R., Kumar, A.: ‘An efficient method for D-STATCOM placement in radial distribution system’, in ‘Power Electronics (IICPE), 2014 IEEE 6th India International Conference on’ (2014), pp. 1–6

[11] Dehnavi, H.D., Esmaeili, S.: ‘A new multiobjective fuzzy shuffled frog-leaping algorithm for optimal reconfiguration of radial distribution systems in the presence of reactive

power compensators'Turkish J. Electr. Eng. Comput. Sci., 2013, 21, (3), pp. 864–881.

[12] Taher, S.A., Afsari, S.A.: 'Optimal location and sizing of DSTATCOM in distribution systems by immune algorithm'Int. J. Electr. Power Energy Syst., 2014, 60, pp. 34–44.

[13] Sheng Xiaoguang, Tongzhen Wei, Qunhai Huo: 'Optimal configuration of multi-DFACTS joint operation in distributed network', in '2014 IEEE Conference and Expo Transportation Electrification Asia-Pacific (ITEC Asia-Pacific)' (2014), pp. 1–5

[14] T. Yuvaraj, K. Ravi, K.R.D.: 'DSTATCOM allocation in distribtuion networks considering load variations using bat algorithm'Ain Shams Eng. J., 2015, pp. 1–13.

[15] Kersting, W.H.: 'Distribution System Modeling and Analysis, Third Edition' (Taylor & Francis, 2012)

[16] Teng, J.-H.: 'A direct approach for distribution system load flow solutions'IEEE Trans. Power Deliv., 2003, 18, pp. 882 – 887.

Appendix

Table A1: Load data of 25-bus system

SB	RB	Branch no	Line code	Branch Length (feet)	Complex load demand		
					Phase A	Phase B	Phase C
1	2	1	1	1000	0	0	0
2	3	2	1	500	35 + j25	40 + j30	45 + j32
2	6	3	2	500	40 + j30	45 + j32	35 + j25
3	4	4	1	500	50 + j40	60 + j45	50 + j35
3	18	5	2	500	40 + j30	40 + j30	40 + j30
4	5	6	2	500	40 + j30	40 + j30	40 + j30
4	23	7	2	400	60 + j45	50 + j40	50 + j35
6	7	8	2	500	0	0	0
6	8	9	2	1000	40 + j30	40 + j30	40 + j30
7	9	10	2	500	60 + j45	50 + j40	50 + j35
7	14	11	2	500	50 + j35	60 + j45	50 + j40
7	16	12	2	500	40 + j30	40 + j30	40 + j30
9	10	13	2	500	35 + j25	40 + j30	45 + j32
10	11	14	2	300	45 + j32	35 + j25	40 + j30
11	12	15	3	200	50 + j35	60 + j45	50 + j40
11	13	16	3	200	35 + j25	45 + j32	40 + j30
14	15	17	2	300	133.3 + j100	133.3 + j100	133.3 + j100
14	17	18	3	300	40 + j30	35 + j32	45 + j32
18	20	19	2	500	35 + j25	40 + j30	45 + j32
18	21	20	3	400	40 + j30	35 + j25	45 + j32
20	19	21	3	400	60 + j45	50 + j35	50 + j40
21	22	22	3	400	50 + j35	60 + j45	50 + j35
23	24	23	2	400	35 + j25	45 + j32	40 + j30
24	25	24	3	400	60 + j45	50 + j30	50 + j35

Table A2: Different types of conductor used in the 25-bus system

Conductor type	25-bus system	
	Self-impedance (Ω/mile)	Mutual impedance (Ω/mile)
1 (3-ϕ)	*Zaa* = 0.3686+j0.6852 *Zbb* = 0.3757+j0.6715 *Zcc* = 0.3723+j0.6782	*Zab* = 0.0169+j0.1515 *Zbc* = 0.0188+j0.2072 *Zca* = 0.0155+j0.1098
2 (3-ϕ)	*Zaa* = 0.9775 + j0.8717 *Zbb* = 0.9844 + j0.8654 *Zcc* = 0.9810 + j0.8648	*Zab* = 0.0167 + j0.1697 *Zbc* = 0.0186 + j0.2275 *Zca* = 0.0152 + j0.1264
3 (3-ϕ)	*Zaa* = 1.9280 + j1.4194 *Zbb* = 1.9308 + j1.4215 *Zcc* = 1.9337 + j1.4236	*Zab* = 0.0161 + j0.1183 *Zbc* = 0.0161 + j0.1183 *Zca* = 0.0161 + j0.1183

Table A3: Load data of 19-bus system

SB	RB	Branch no	Line code	Branch Length (km)	Base case complex load demand		
1	2	1	1	3.0	10.38+j5.01	5.19+j2.52	10.38+j5.01
2	3	2	1	5.0	11.01+j5.34	5.19+j2.52	9.72+j4.71
3	4	3	1	1.5	4.05+j1.95	5.67+j2.76	6.48+j3.15
4	5	4	1	1.5	6.48 + j3.15	5.19+j2.52	4.53+j2.19
4	6	5	1	1.0	4.20 + j2.04	3.09 + j1.50	2.91 + j1.42
6	7	6	1	2.0	9.72 + j4.71	8.10 + j3.93	8.10 + j3.93
6	8	7	1	2.5	7.44 + j3.60	5.34 + j2.58	3.39 + j1.65
8	9	8	1	3.0	12.30 + j5.97	14.91 + j7.23	13.29 + j6.42
9	10	9	1	5.0	3.39 + j1.65	4.20 + j2.04	2.58 + j1.26
10	11	10	1	1.5	7.44 + j3.60	7.44 + j3.60	11.01 + j5.34
10	12	11	1	1.5	9.72 + j4.71	8.10 + j3.93	8.10 + j3.93
11	13	12	1	5.0	4.38 + j2.13	5.34 + j2.58	6.48 + j3.15
11	14	13	1	1.0	3.09 + j1.50	3.09 + j1.50	4.05 + j1.95
12	15	14	1	5.0	4.38 + j2.13	4.86 + j2.34	6.96 + j3.36
12	16	15	1	6.0	7.77 + j3.78	10.38 + j5.01	7.77 + j3.78
14	17	16	1	3.5	6.48 + j3.12	4.86 + j2.34	4.86 + j2.34
14	18	17	1	4.0	5.34 + j2.58	5.34 + j2.58	5.52 + j2.67
15	19	18	1	4.0	8.76 + j4.23	10.05+ j4.86	7.14 + j3.45

Table A4: Different types of conductor used in the 19-bus system

Conductor type	19-bus system	
	Self-impedance (Ω/km)	Mutual impedance (Ω/km)
1 (3-ϕ)	*Zaa* = 1.5609+j0.67155 *Zbb* = 1.5609+j0.67155 *Zcc* = 1.5609+j0.67155	*Zab* = 0.5203+j0.22385 *Zbc* = 0.5203+j0.22385 *Zca* = 0.5203+j0.22385